Z_2 Topological Order and the Quantum Spin Hall Effect

C. L. Kane and E. J. Mele

Department of Physics and Astronomy, University of Pennsylvania, Philadelphia, Pennsylvania 19104, USA

(Received 22 June 2005; published 28 September 2005)

The quantum spin Hall (QSH) phase is a time reversal invariant electronic state with a bulk electronic band gap that supports the transport of charge and spin in gapless edge states. We show that this phase is associated with a novel Z_2 topological invariant, which distinguishes it from an ordinary insulator. The Z_2 classification, which is defined for time reversal invariant Hamiltonians, is analogous to the Chern number classification of the quantum Hall effect. We establish the Z_2 order of the QSH phase in the two band model of graphene and propose a generalization of the formalism applicable to multiband and interacting systems.

DOI: 10.1103/PhysRevLett.95.146802 PACS numbers: 73.43.−f, 72.25.Hg, 73.61.Wp, 85.75.−d

The classification of electronic states according to topological invariants is a powerful tool for understanding many body phases which have bulk energy gaps. This approach was pioneered by Thouless, Kohmoto, Nightingale, and den Nijs [1] (TKNN), who identified the topological invariant for the noninteracting integer quantum Hall effect. The TKNN integer, n, which gives the quantized Hall conductivity for each band $\sigma_{xy} = ne^2/h$, is given by an integral of the Bloch wave functions over the magnetic Brillouin zone, and corresponds to the first Chern class of a $U(1)$ principal fiber bundle on a torus [2,3]. An equivalent formulation, generalizable to interacting systems, is to consider the sensitivity of the many body ground state to phase twisted periodic boundary conditions [4,5]. This topological classification distinguishes a simple insulator from a quantum Hall state, and explains the insensitivity of the Hall conductivity to weak disorder and interactions. Nonzero TKNN integers are also intimately related to the presence of gapless edge states on the sample boundaries [6].

Since the Hall conductivity violates time reversal ($\mathcal{T}$) symmetry, the TKNN integer must vanish in a $\mathcal{T}$-invariant system. Nonetheless, we have recently shown that the spin-orbit interaction in a single plane of graphene leads to a $\mathcal{T}$-invariant quantum spin Hall (QSH) state which has a bulk energy gap, and a pair of gapless spin filtered edge states on the boundary [7]. In the simplest version of our model (a π-electron tight-binding model with mirror-symmetry about the plane) the perpendicular component of the spin, S_z, is conserved. Our model then reduces to independent copies for each spin of a model introduced by Haldane [8], which exhibits an integer quantum Hall effect even though the average magnetic field is zero. When S_z is conserved the distinction between graphene and a simple insulator is thus easily understood. Each spin has an independent TKNN integer $n_\uparrow$, $n_\downarrow$. $\mathcal{T}$ symmetry requires $n_\uparrow + n_\downarrow = 0$, but the difference $n_\uparrow - n_\downarrow$ is nonzero and defines a quantized spin Hall conductivity.

This characterization breaks down when S_z nonconserving terms are present. Such terms will inevitably arise due to coupling to other bands, mirror-symmetry breaking terms, interactions, or disorder. Though these perturbations destroy the quantization of the spin Hall conductance, we argued that they do not destroy the topological order of the QSH state because Kramers' theorem prevents $\mathcal{T}$-invariant perturbations from opening a gap at the edge [7]. Thus, even though the single defined TKNN number (the total Hall conductance) is zero, the QSH ground state is distinguishable from that of a simple insulator. This suggests that there must be an additional topological classification for $\mathcal{T}$-invariant systems.

In this Letter we clarify the topological order of the QSH phase and introduce a Z_2 topological index that characterizes $\mathcal{T}$-invariant systems. This classification is similar to the TKNN classification, and gives a simple test which can be applied to Bloch energy bands to distinguish the insulator from the QSH phase. It may also be formulated as a sensitivity to phase twisted boundary conditions. We will begin by describing our model of graphene and demonstrate that the QSH phase is robust even when S_z is not conserved. We will then analyze the constraints of $\mathcal{T}$ invariance and derive the Z_2 index.

Consider the tight-binding Hamiltonian of graphene introduced in Ref. [7], which generalizes Haldane's model [8] to include spin with $\mathcal{T}$-invariant spin-orbit interactions.

$$H = t\sum_{\langle ij\rangle} c_i^\dagger c_j + i\lambda_{\mathrm{SO}} \sum_{\langle\langle ij\rangle\rangle} \nu_{ij} c_i^\dagger s^z c_j + i\lambda_R \sum_{\langle ij\rangle} c_i^\dagger (\mathbf{s}\times\hat{\mathbf{d}}_{ij})_z c_j + \lambda_v \sum_i \xi_i c_i^\dagger c_i. \quad (1)$$

The first term is a nearest neighbor hopping term on the honeycomb lattice, where we have suppressed the spin index on the electron operators. The second term is the mirror symmetric spin-orbit interaction which involves spin dependent second neighbor hopping. Here $\nu_{ij} = (2/\sqrt{3})(\hat{\mathbf{d}}_1 \times \hat{\mathbf{d}}_2)_z = \pm 1$, where $\hat{\mathbf{d}}_1$ and $\hat{\mathbf{d}}_2$ are unit vectors along the two bonds the electron traverses going from site j to i. s^z is a Pauli matrix describing the electron's spin. The third term is a nearest neighbor Rashba term, which explicitly violates the $z \to -z$ mirror symmetry, and will

arise due to a perpendicular electric field or interaction with a substrate. The fourth term is a staggered sublattice potential ($\xi_i = \pm 1$), which we include to describe the transition between the QSH phase and the simple insulator. This term violates the symmetry under twofold rotations in the plane.

H is diagonalized by writing $\phi_s(\mathbf{R} + \alpha\mathbf{d}) = u_{\alpha s}(\mathbf{k})e^{i\mathbf{k}\cdot\mathbf{R}}$. Here s is spin and $\mathbf{R}$ is a bravais lattice vector built from primitive vectors $\mathbf{a}_{1,2} = (a/2)(\sqrt{3}\hat{\mathbf{y}} \pm \hat{\mathbf{x}})$. $\alpha = 0, 1$ is the sublattice index with $\mathbf{d} = a\hat{\mathbf{y}}/\sqrt{3}$. For each $\mathbf{k}$ the Bloch wave function is a four component eigenvector $|u(\mathbf{k})\rangle$ of the Bloch Hamiltonian matrix $\mathcal{H}(\mathbf{k})$. The 16 components of $\mathcal{H}(\mathbf{k})$ may be written in terms of the identity matrix, 5 Dirac matrices Γ^a and their 10 commutators $\Gamma^{ab} = [\Gamma^a, \Gamma^b]/(2i)$ [9]. We choose the following representation of the Dirac matrices: $\Gamma^{(1,2,3,4,5)} = (\sigma^x \otimes I, \sigma^z \otimes I, \sigma^y \otimes s^x, \sigma^y \otimes s^y, \sigma^y \otimes s^z)$, where the Pauli matrices σ^k and s^k represent the sublattice and spin indices. This choice organizes the matrices according to $\mathcal{T}$. The $\mathcal{T}$ operator is given by $\Theta|u\rangle \equiv i(I \otimes s^y)|u\rangle^*$. The five Dirac matrices are even under $\mathcal{T}$, $\Theta\Gamma^a\Theta^{-1} = \Gamma^a$ while the 10 commutators are odd, $\Theta\Gamma^{ab}\Theta^{-1} = -\Gamma^{ab}$. The Hamiltonian is thus

$$\mathcal{H}(\mathbf{k}) = \sum_{a=1}^{5} d_a(\mathbf{k})\Gamma^a + \sum_{a<b=1}^{5} d_{ab}(\mathbf{k})\Gamma^{ab}, \qquad (2)$$

where the $d(\mathbf{k})$'s are given in Table I. Note that $\mathcal{H}(\mathbf{k} + \mathbf{G}) = \mathcal{H}(\mathbf{k})$ for reciprocal lattice vectors $\mathbf{G}$, so $\mathcal{H}(\mathbf{k})$ is defined on a torus. The $\mathcal{T}$ invariance of $\mathcal{H}$ is reflected in the symmetry (antisymmetry) of d_a (d_{ab}) under $\mathbf{k} \rightarrow -\mathbf{k}$.

Equation (2) gives four energy bands, of which two are occupied. For $\lambda_R = 0$ there is an energy gap with magnitude $|6\sqrt{3}\lambda_{\mathrm{SO}} - 2\lambda_v|$. For $\lambda_v > 3\sqrt{3}\lambda_{\mathrm{SO}}$ the gap is dominated by λ_v, and the system is an insulator. $3\sqrt{3}\lambda_{\mathrm{SO}} > \lambda_v$ describes the QSH phase. Though the Rashba term violates S_z conservation, for $\lambda_R < 2\sqrt{3}\lambda_{\mathrm{SO}}$ there is a finite region of the phase diagram in Fig. 1 that is adiabatically connected to the QSH phase at $\lambda_R = 0$. Figure 1 shows the energy bands obtained by solving the lattice model in a zigzag strip geometry [7] for representative points in the insulating and QSH phases. Both phases have a bulk energy gap and edge states, but in the QSH phase the edge states traverse the energy gap in pairs. At the transition between the two phases, the energy gap closes, allowing the edge states to "switch partners."

The behavior of the edge states signals a clear difference between the two phases. In the QSH phase for each energy in the bulk gap there is a single time reversed pair of eigenstates on each edge. Since $\mathcal{T}$ symmetry prevents the mixing of Kramers' doublets these edge states are robust against small perturbations. The gapless states thus persist even if the spatial symmetry is further reduced [for instance, by removing the C_3 rotational symmetry in (1)]. Moreover, weak disorder will not lead to localization of the edge states because single particle elastic backscattering is forbidden [7].

In the insulating state the edge states do not traverse the gap. It is possible that for certain edge potentials the edge states in Fig. 1(b) could dip below the band edge, reducing—or even eliminating—the edge gap. However, this is still distinct from the QSH phase because there will necessarily be an *even* number of Kramers' pairs at each energy. This allows elastic backscattering, so that these edge states will in general be localized by weak disorder. The QSH phase is thus distinguished from the simple insulator by the number of edge state pairs modulo 2. Recently two-dimensional versions [10] of the spin Hall insulator models [11] have been introduced, which under conditions of high spatial symmetry exhibit gapless edge states. These models, however, have an even number of edge state pairs. We shall see below that they are topologically equivalent to simple insulators.

The QSH phase is *not* generally characterized by a quantized spin Hall conductivity. Consider the rate of spin accumulation at the opposite edges of a cylinder of circumference L, which can be computed using Laughlin's argument [12]. A weak circumferential electric field E can be induced by adiabatically threading magnetic flux through the cylinder. When the flux increases by h/e each momentum eigenstate shifts by one unit: $k \rightarrow k + 2\pi/L$. In the insulating state [Fig. 1(b)] this has no effect, since the valence band is completely full. However, in the QSH state a particle-hole excitation is produced at the Fermi energy E_F. Since the particle and hole states do not have the same spin, spin accumulates at the edge. The rate of spin accumulation defines a spin Hall conductance $d\langle S_z\rangle/dt = G^s_{xy}E$, where

TABLE I. The nonzero coefficients in Eq. (2) with $x = k_x a/2$ and $y = \sqrt{3}k_y a/2$.

d_1	$t(1 + 2\cos x \cos y)$	d_{12}	$-2t\cos x \sin y$
d_2	λ_v	d_{15}	$\lambda_{\mathrm{SO}}(2\sin 2x - 4\sin x \cos y)$
d_3	$\lambda_R(1 - \cos x \cos y)$	d_{23}	$-\lambda_R \cos x \sin y$
d_4	$-\sqrt{3}\lambda_R \sin x \sin y$	d_{24}	$\sqrt{3}\lambda_R \sin x \cos y$

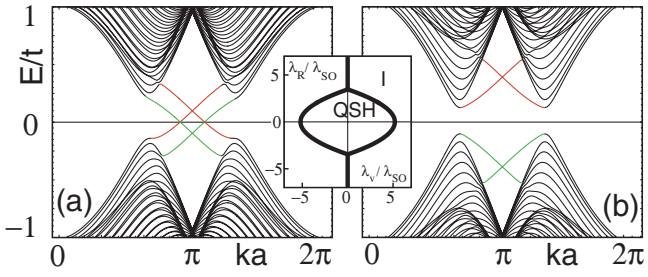

FIG. 1 (color online). Energy bands for a one-dimensional "zigzag" strip in the (a) QSH phase $\lambda_v = 0.1t$ and (b) the insulating phase $\lambda_v = 0.4t$. In both cases $\lambda_{\mathrm{SO}} = .06t$ and $\lambda_R = .05t$. The edge states on a given edge cross at $ka = \pi$. The inset shows the phase diagram as a function of λ_v and λ_R for $0 < \lambda_{\mathrm{SO}} \ll t$.

$$G^s_{xy} = \frac{e}{h}(\langle S_z\rangle_L - \langle S_z\rangle_R)|_{E_F}. \quad (3)$$

Here the expectation value of S_z is evaluated for the left and right moving states at E_F. Since the edge states are not necessarily S_z eigenstates this spin Hall conductance is not quantized. G^s_{xy} is zero in the insulating phase, though, provided E_F is in the gap at the edge. If in the insulator the edge states cross E_F, then in a clean system there could be spin accumulation at the edge (resulting from the acceleration of the edge electrons in response to E). However, if the edge states are localized then there will be no spin accumulation. Thus the nonzero spin accumulation persists only for the QSH phase, justifying the term quantum (but not quantized) spin Hall effect.

In the quantum Hall effect, the states with zero and one flux quantum threading the cylinder are distinguished by the charge polarization. The two states cannot be connected by any operator that locally conserves charge. In the QSH effect there is no simple conserved quantity distinguishing the two states. However, the states *are* distinguishable, because the state with an edge particle-hole excitation at E_F cannot be connected to the ground state with a local $\mathcal{T}$ symmetric operator. Note, however, that if a second flux is added, then there will be $\mathcal{T}$ invariant interactions which do connect the state with the zero flux state. This suggests that the state with one flux added is distinguished by a Z_2 "$\mathcal{T}$ polarization."

The classification of quantum Hall states on the cylinder according to Laughlin's argument is intimately related to the TKNN classification of the Bloch wave functions [4]. To establish the corresponding topological classification for $\mathcal{T}$-invariant systems we consider $\mathcal{T}$ constraints on the Bloch wave functions for the two occupied bands $|u_{i=1,2}(\mathbf{k})\rangle$. $|u_i(\mathbf{k})\rangle$ form a rank 2 vector bundle over Brillouin zone torus. $\mathcal{T}$ introduces an involution on the torus which identifies pairs of points $\mathbf{k}$ and $-\mathbf{k}$. Wave functions at the identified points are related by $|u_i(-\mathbf{k})\rangle = \Theta|u_i(\mathbf{k})\rangle$, implying that the bundle is "real." Since $\Theta^2 = -1$, Θ has period 4, so that the real bundle is "twisted." These bundles are classified within the mathematical framework of twisted Real K theory [13]. It is found that such bundles have a $Z \times Z_2$ classification on a torus [14]. The first integer gives the rank of the bundle (i.e., the number of occupied bands). The Z_2 index is related to the mod 2 index of the real Dirac operator [15]. In the following we will explicitly construct this Z_2 index from the Bloch wave functions and show that it distinguishes the QSH phase from the simple insulator.

$\mathcal{T}$ symmetry identifies two important subspaces of the space of Bloch Hamiltonians $\mathcal{H}(\mathbf{k})$ and the corresponding occupied band wave functions $|u_i(\mathbf{k})\rangle$. The "even" subspace, for which $\Theta H(\mathbf{k})\Theta^{-1} = H(\mathbf{k})$, have the property that $\Theta|u_i(\mathbf{k})\rangle$ is equivalent to $|u_i(\mathbf{k})\rangle$ up to a $U(2)$ rotation. From Eq. (2) it is clear that in this subspace $d_{ab}(\mathbf{k}) = 0$. $\mathcal{T}$ symmetry requires that $H(\mathbf{k})$ belong to the even subspace at the Γ point $\mathbf{k} = \mathbf{0}$ as well as the three M points shown in Figs. 2(a) and 2(b). The odd subspace has wave functions with the property that the space spanned by $\Theta|u_i(\mathbf{k})\rangle$ is *orthogonal* to the space spanned by $|u_i(\mathbf{k})\rangle$. We will establish the Z_2 classification by studying the set of $\mathbf{k}$ which belong to the odd subspace.

The special subspaces can be identified by considering the matrix of overlaps, $\langle u_i(\mathbf{k})|\Theta|u_j(\mathbf{k})\rangle$. From the properties of Θ it is clear that this matrix is antisymmetric, and may be expressed in terms of a single complex number as $\epsilon_{ij}P(\mathbf{k})$. $P(\mathbf{k})$ is in fact equal to the *Pfaffian*

$$P(\mathbf{k}) = \mathrm{Pf}\,[\langle u_i(\mathbf{k})|\Theta|u_j(\mathbf{k})\rangle], \quad (4)$$

which for a 2×2 antisymmetric matrix A_{ij} simply picks out A_{12}. We shall see below that the Pfaffian is the natural generalization when there are more than two occupied bands. $P(\mathbf{k})$ is not gauge invariant. Under a $U(2)$ transformation $|u'_i\rangle = U_{ij}|u_j\rangle$, $P' = P\,\mathrm{det}U$. Thus P is unchanged by a $SU(2)$ rotation, but under a $U(1)$ transformation $U = e^{i\theta}$, $P' = Pe^{2i\theta}$. In the even subspace $\Theta|u_i\rangle$ is equivalent to $|u_i\rangle$ up to a $U(2)$ rotation, and we have $|P(\mathbf{k})| = 1$. In the odd subspace $P(\mathbf{k}) = 0$.

If no spatial symmetries constrain its form, the zeros of $P(\mathbf{k})$ are found by tuning two parameters, and generically occur at points in the Brillouin zone. First order zeros occur at time reversed pairs of points $\pm\mathbf{k}^*$ with opposite "vorticity," where the phase of $P(\mathbf{k})$ advances in opposite directions around $\pm\mathbf{k}^*$. For $\lambda_v \neq 0$ the QSH phase is distinguished from the simple insulator by the presence of a single pair of first order zeros of $P(\mathbf{k})$. The C_3 rotational symmetry of our model constrains $\mathbf{k}^*$ to be at the corner of the Brillouin zone as shown in Fig. 2(a). If the C_3 symmetry is relaxed, $\mathbf{k}^*$ can occur anywhere *except* the

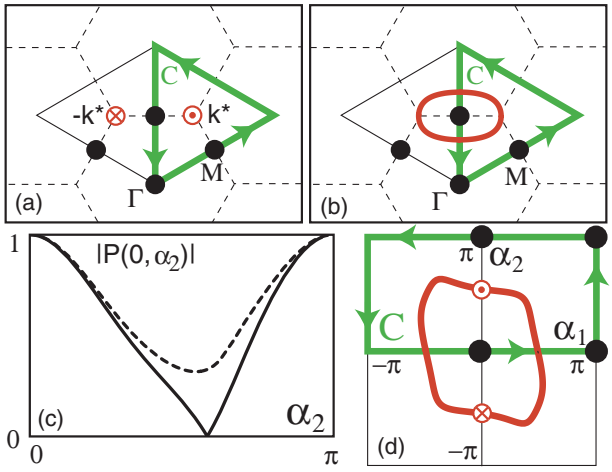

FIG. 2 (color online). The zeros of $P(\mathbf{k})$ in the QSH phase occur at points $\pm\mathbf{k}^*$ for (a) $\lambda_v \neq 0$ and on the oval for (b) $\lambda_v = 0$. (c) $|P(0, \alpha_2)|$ in the QSH (solid line) and insulating (dashed line) phases for a 2×2 supercell using parameters in Fig. 1. (d) Point ($\lambda_v \neq 0$) and line ($\lambda_v = 0$) zeros of $P(\vec{\alpha})$ for the 2×2 supercell. In (a), (b), and (d) the solid dots are $\mathcal{T}$-symmetric points, which cannot be zeros of P, and C is the contour of integration for Eq. (5).

four symmetric points where $|P(\mathbf{k})| = 1$. The number of pairs of zeros is a Z_2 topological invariant. This can be seen by noting that two pairs $\pm\mathbf{k}^*_{1,2}$ can come together to annihilate each other when $\mathbf{k}^*_1 = -\mathbf{k}^*_2$. However a single pair of zeros at $\pm\mathbf{k}^*$ cannot annihilate because they would have to meet at either Γ or M, where $|P(\mathbf{k})| = 1$. If $\mathcal{T}$ symmetry is broken then the zeros are no longer prevented from annihilating, and the topological distinction of the QSH phase is lost.

The Z_2 index can thus be determined by counting the number of pairs of complex zeros of P. This can be accomplished by evaluating the winding of the phase of $P(\mathbf{k})$ around a loop enclosing *half* the Brillouin zone (defined so that $\mathbf{k}$ and $-\mathbf{k}$ are never both included).

$$I = \frac{1}{2\pi i}\oint_C d\mathbf{k}\cdot\nabla_{\mathbf{k}}\log[P(\mathbf{k}) + i\delta], \tag{5}$$

where C is the path shown in Figs. 2(a) and 2(b).

When $\lambda_v = 0$ (as it is in graphene) H has a C_2 rotational symmetry, which when combined with $\mathcal{T}$ constrains the form of $\mathcal{H}(\mathbf{k})$, and allows $P(\mathbf{k})$ to be chosen to be real. The zeros of $P(\mathbf{k})$ then occur along lines, rather than at points. We find that the zeros are absent in the insulating phase, but enclose the M point in the QSH phase as shown in Fig. 2(b). In this case we find that Eq. (4) also determines the Z_2 index (given by $1/2$ the number of sign changes along the path C), provided we include the convergence factor δ. Note that though the sign of I depends on the sign of δ, I mod 2 does not. We thus conclude that the QSH phase and the insulator are distinguished by the Z_2 index I.

The spin Hall insulator models studied in Refs. [10,11] are simple insulators with $I = 0$. Their Hamiltonian, when expressed in the form of Eq. (2), has $d_{ab}(\mathbf{k}) = 0$, so that $|u_i(\mathbf{k})\rangle$ is in the even subspace and $|P(\mathbf{k})| = 1$ for all $\mathbf{k}$. Reference [16] introduces a model which does appear to exhibit a QSH effect.

Having established the topological classification of the Bloch wave functions we now ask whether, in analogy with Ref. [4], the classification can be formulated in terms of the sensitivity of the ground state wave function to phase twisted periodic boundary conditions. Such a formulation will address the topological stability of the many body ground state with respect to weak disorder and electron interactions. It also provides the appropriate generalization of (4) and (5) for multiband Hamiltonians. Consider a $\mathbf{L}_1 \times \mathbf{L}_2$ sample with boundary condition $\Psi(\ldots, \mathbf{r}_i + \mathbf{L}_k, \ldots) = e^{i\alpha_k}\Psi(\ldots, \mathbf{r}_i, \ldots)$. For concreteness we consider a rectangular geometry, with $\mathbf{L}_1 = N_1(\mathbf{a}_1 + \mathbf{a}_2)$ and $\mathbf{L}_2 = N_2(\mathbf{a}_1 - \mathbf{a}_2)$. For noninteracting electrons, we may view the entire sample as a large unit cell with $N_a = 4N_1N_2$ atoms imbedded in an even larger crystal. Then $\vec{\alpha}$ plays the role of $\mathbf{k}$, and the occupied single particle eigenstates $\phi_i(\vec{\alpha})$ play the role of $u_i(\mathbf{k})$. $\phi_i(\vec{\alpha})$ form a rank N_a bundle on the torus defined by $\alpha_{1,2}$. The Z_2 classification can be obtained by studying the zeros of

$$P(\vec{\alpha}) = \mathrm{Pf}\,[\langle\phi_i(\vec{\alpha})|\Theta|\phi_j(\vec{\alpha})\rangle]. \tag{6}$$

Figure 2(c) compares $|P(\vec{\alpha})|$ in the QSH and insulating phases. For a 16-site sample with $N_1 = N_2 = 2$. In the insulating phase there are no zeros. In the QSH phase the structure of the zeros in Fig. 2(d) is similar to Figs. 2(a) and 2(b). For $\lambda_v \neq 0$ the first order zeros are at points, while for $\lambda_v = 0$ they are on a loop. The zeros cannot be at the four $\mathcal{T}$ symmetric points. This structure persists in the QSH phase for any cell size. The Z_2 index I can be computed by performing the integral analogous to (5) along the contour C in Fig. 2(d).

A many body formulation requires the index to be expressed in terms of the many particle ground state $|\Phi(\vec{\alpha})\rangle$. It is interesting to note that for noninteracting electrons $\langle\Phi(\vec{\alpha})|\Theta|\Phi(\vec{\alpha})\rangle = \det[\langle\phi_i(\vec{\alpha})|\Theta|\phi_j(\vec{\alpha})\rangle] = P(\vec{\alpha})^2$. This suggests a many body generalization

$$P(\vec{\alpha}) = \sqrt{\langle\Phi(\vec{\alpha})|\Theta|\Phi(\vec{\alpha})\rangle}. \tag{7}$$

We suspect that with this definition the topological structure $P(\vec{\alpha})$ in Figs. 2(c) and 2(d) will remain in the presence of weak electron interactions.

To conclude, we have introduced a Z_2 topological classification of $\mathcal{T}$ invariant systems, analogous to the TKNN classification of quantum Hall states. This shows that the QSH phase of graphene has a topological stability that is insensitive to weak disorder and interactions.

We thank Tony Pantev for many helpful discussions. This work was supported by the NSF under MRSEC Grant No. DMR-00-79909 and the DOE under Grant No. DE-FG02-ER-0145118.

[1] D. J. Thouless, M. Kohmoto, M. P. Nightingale, and M. den Nijs, Phys. Rev. Lett. **49**, 405 (1982).
[2] J. E. Avron, R. Seiler, and B. Simon, Phys. Rev. Lett. **51**, 51 (1983).
[3] M. Kohmoto, Ann. Phys. (Berlin) **160**, 343 (1985).
[4] Q. Niu, D. J. Thouless, and Y. S. Wu, Phys. Rev. B **31**, 3372 (1985).
[5] D. P. Arovas *et al.*, Phys. Rev. Lett. **60**, 619 (1988).
[6] Y. Hatsugai, Phys. Rev. Lett. **71**, 3697 (1993).
[7] C. L. Kane and E. J. Mele, cond-mat/0411737.
[8] F. D. M. Haldane, Phys. Rev. Lett. **61**, 2015 (1988).
[9] S. Murakami, N. Nagaosa, and S. C. Zhang, Science **301**, 1348 (2003); Phys. Rev. B **69**, 235206 (2004).
[10] X. L. Qi, Y. S. Wu, and S. C. Zhang, cond-mat/0505308; M. Onoda and N. Nagaosa, Phys. Rev. Lett. **95**, 106601 (2005).
[11] S. Murakami, N. Nagaosa, and S. C. Zhang, Phys. Rev. Lett. **93**, 156804 (2004).
[12] R. B. Laughlin, Phys. Rev. B **23**, R5632 (1981).
[13] M. Atiyah, Quart. J. Math. Oxford **17**, 367 (1966); M. Atiyah and G. Segal, in *Michael Atiyah Collected Works* (Clarendon, Oxford, 2004), Vol. 6, p. 983.
[14] We are indebted to Tony Pantev for explaining these connections to us.
[15] M. Atiyah and I. Singer, Ann. Math. **93**, 139 (1971).
[16] B. A. Bernevig and S. C. Zhang, cond-mat/0504147.